Molecular Crystals and Liquid Crystals
Publication details, including instructions for authors and subscription information:
http://www.tandfonline.com/loi/gmcl16

Resistivity, Permittivity and the Electrode Space Charge of Nematic Liquid Crystals

G. J. Sprokel [a]
[a] IBM System Products Division, East Fishkill Facility, Hopewell Junction, New York, 12533
Version of record first published: 21 Mar 2007.

To cite this article: G. J. Sprokel (1973): Resistivity, Permittivity and the Electrode Space Charge of Nematic Liquid Crystals, Molecular Crystals and Liquid Crystals, 22:3-4, 249-260

To link to this article: http://dx.doi.org/10.1080/15421407308083348

Molecular Crystals and Liquid Crystals. 1973. Vol. 22, pp. 249–260

Printed in Great Britain

Resistivity, Permittivity and the Electrode Space Charge of Nematic Liquid Crystals†

G. J. SPROKEL

IBM System Products Division
East Fishkill Facility
Hopewell Junction, New York 12533

Received November 7, 1972

Abstract—The permittivity of doped nematics is found to increase approximately as $(1/\omega)^2$ at low frequency. The effect is accounted for by considering the space charge resulting from dissociation of the dopant. The space charge capacitance is obtained from experimental data and compared with that of a simple model.

1. Introduction

A liquid crystal display cell can be regarded as a parallel plate capacitor filled with a—rather leaky—dielectric. The RC time constant is readily estimated from published data. Thus if ϵ is of the order of 5 (Diguet *et al.*[1]) and ρ is of the order of 10^{10} ohm cm[2,3] the time constant $\epsilon_0 \epsilon \rho$ is of the order of 5×10^{-3} sec.

A well-known method to determine R and C of a parallel network is to put it in series with a known network (R_s, C_s) and apply a square wave pulse longer than the time constant. C_s is adjusted until the output reproduces the input wave shape. If this simple experiment is performed with a liquid crystal cell it is found that C_s cannot be adjusted to make the output resemble a square wave which implies that the liquid crystal cell is not a parallel RC circuit. Changing the input signal to a sine wave one can indeed balance out the phase difference between input and output but one finds that C_s has to be increased if the frequency of the input is decreased. The cell resistance is found to be independent of frequency. Electrical parameters are important to circuit designers. The frequency dependence of the cell capacitance is of interest in its own right and forms the subject of this paper.

† Paper presented at the 4th International Liquid Crystal Conference, Kent State University, August 1972.

2. Experimental Procedures

The series circuit described above is unsuitable for accurate measurements. The stray capacitance at the junction is unknown and in fact larger than the cell capacitance. The cell resistance can only be determined to about 10% accuracy. These problems are eliminated in a bridge circuit. A direct coupled bridge designed for low frequency (0–10 kHz) measurements on doped nematics was constructed. Details of the instrument have already been discussed.[4] The instrument in effect substitutes the electrical parameters of the test cell with those of a parallel *RC* network.

Test cells are made by evaporating a suitable conductor such as Cr, Al or In_2O_3 on a flat glass surface. The electrode pattern, a 0.500 in. diameter circle and a 0.010 in. connecting line, is etched by standard photolithography. Two plates are bonded together using 0.001 in. polyimid spacers. The cell is mounted in an aluminum box continuously flushed with dry nitrogen. The box can be inserted between the poles of a Varian magnet using either parallel or crossed E and H fields.

The calculated cell capacitance is 44.3 pF. The measured capacitance is in the 35–45 pF range. The stray capacitance of an empty cell is about 2 pF. Empty cells were used to obtain the reproducibility of the measurement. The standard deviation of a large number of measurements is about 1%.

Materials used to prepare liquid crystal solutions are commercial products (Kodak, Aldrich) recrystallized, dried over P_2O_5 in vacuum and stored in dry nitrogen atmosphere. Even for purified material one often finds that the resistance of a newly filled cell increases by a few percent in the first hour. However, the resistance stabilizes in a few hours and remains within 2% thereafter. A few cells were tested for 2 or 3 weeks and remained constant. Aging effects occurring over many months are not considered here. Commercial liquid crystal material, not recrystallized, shows a continuous change in resistance for several weeks but tends to stabilize eventually.

3. Results

In Fig. 1 the resistivity, ρ, and the apparent permittivity ϵ_{app}

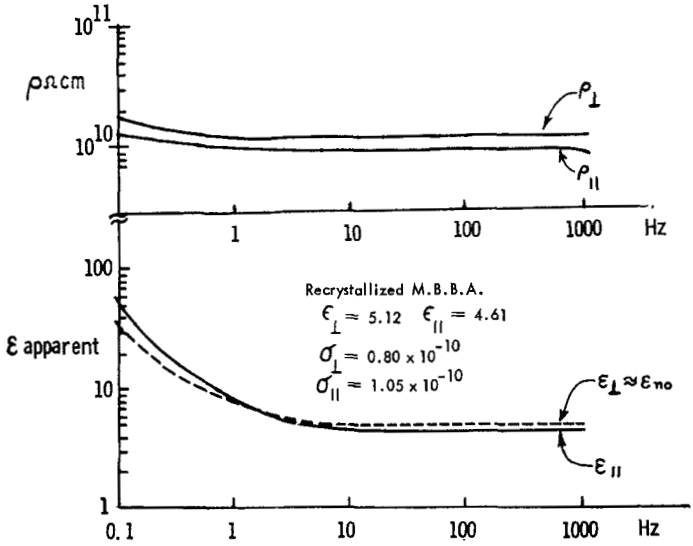

Figure 1. ϵ_{app} and ρ for recrystallized MBBA.
$\epsilon_{||} = 4.61$ $\epsilon_\perp = 5.12$ (50 Hz–1000 Hz)
$\sigma_{||} = 1.05 \times 10^{-10}(\Omega\ \text{cm})^{-1}$ $\sigma_\perp = 0.80 \times 10^{-10}(\Omega\ \text{cm})^{-1}$
C_{el} @ 0.1 Hz $1.5\mu\text{F/cm}^2 \pm 0.2\mu\text{F/cm}^2$
@ 0.2 Hz $1.1\mu\text{F/cm}^2 \pm 0.2\mu\text{F/cm}^2$
Aluminum electrodes. Alignment nearly parallel.

is plotted against the frequency for a sample of recrystallized MBBA. The resistivity is calculated as

$$\rho = \frac{1}{\epsilon_0} RC_v\ \Omega\ \text{cm}$$

where R is the experimental cell resistance and C_v is the capacitance of the empty cell. $\epsilon_0 = 8.854 \times 10^{-14}\ \text{F cm}^{-1}$. ϵ_{app} is the ratio of the capacitance of the filled cell and that of the empty cell, both corrected for stray capacitance.

Figure 2 shows ρ and ϵ_{app} for the same MBBA sample doped with 0.76×10^{-4} mol/mol choline chloride. (The system forms a true solution in the sense that even after long standing no crystalline precipitates can be observed under the polarization microscope.) The indices $||$ and $\perp$ refer to parallel respectively crossed H and E field. In Figs. 1 and 2 data for $H = 0$ practically coincide with the $\epsilon_\perp$ data, i.e., alignment is parallel with the surface.

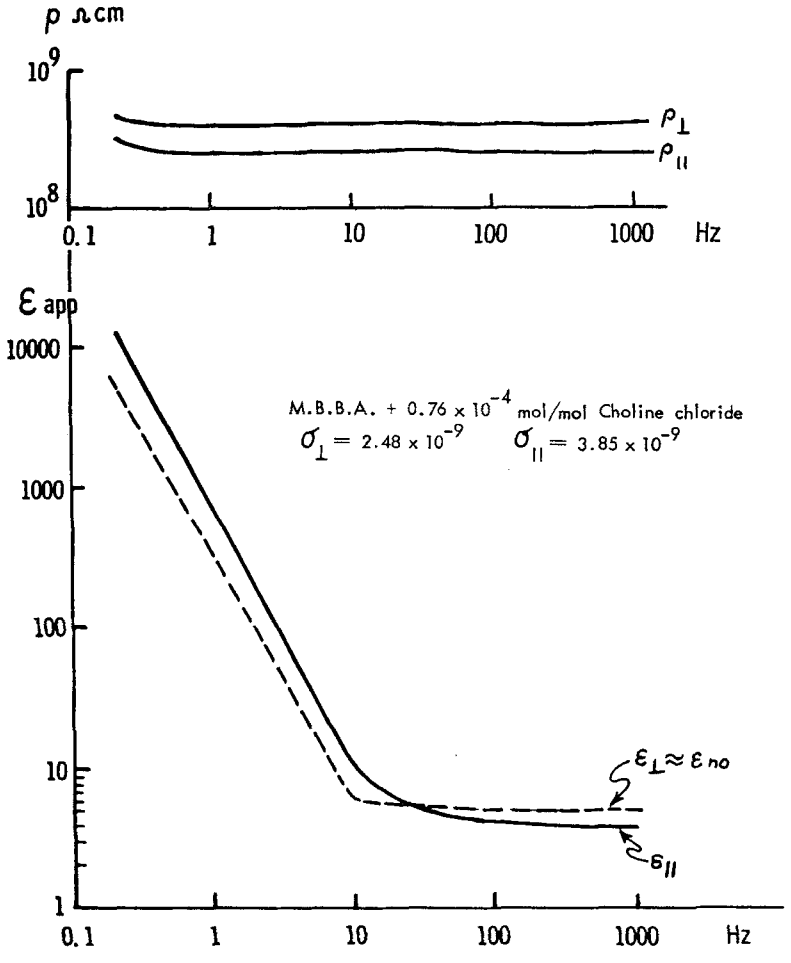

Figure 2. ϵ_{app} and ρ for MBBA doped with 0.76×10^{-4} mol/mol choline chloride.

$\epsilon_{\parallel} = 4.68 \quad \epsilon_{\perp} = 5.12$
$\sigma_{\parallel} = 3.85 \times 10^{-9} \quad \sigma_{\perp} = 2.48 \times 10^{-9} (\Omega\,\mathrm{cm})^{-1}$
C_{el} see text.

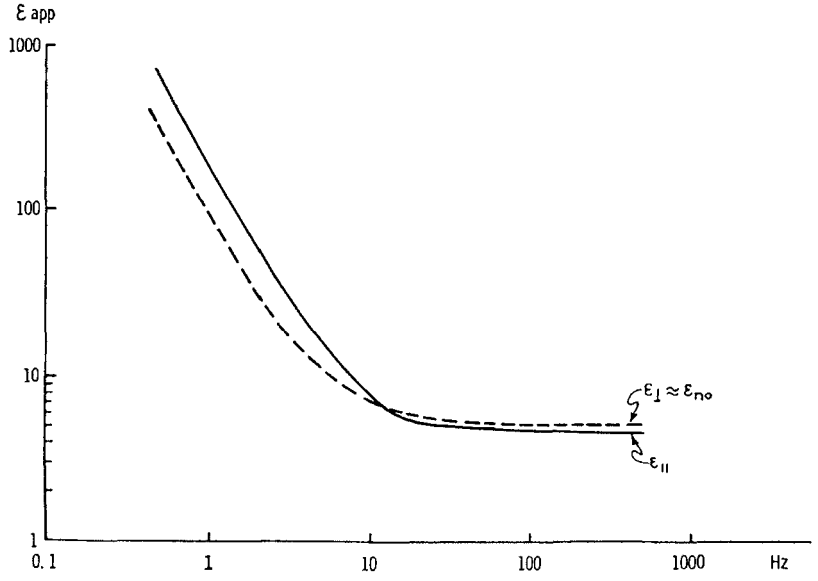

Figure 3. ϵ_{app} and ρ for distilled MBBA doped with 0.92×10^{-4} mol/mol N dodecylpyridinium-*p*-toluene sulfonate.
$\epsilon_{\|} = 4.80$ $\epsilon_{\perp} = 5.43$; $\sigma_{\|} = 1.91 \times 10^{-9}$ $\sigma_{\perp} = 1.28 \times 10^{-9} (\Omega \mathrm{cm})^{-1}$; C_{el} in $\mu F/\mathrm{cm}^2$

Hz	⊥	‖
0.5	2.4	2.5
1	2.1	2.1
2	2.0	2.0

It is seen that the resistivity is constant throughout the range of frequency, below 0.5 Hz there is usually a slight increase. However, ϵ_{app} increases sharply at low frequency, for doped samples the increase is about 3 orders of magnitude. At high frequency ϵ_{app} is constant and $\epsilon_{\|} < \epsilon_{\perp}$ as expected for a negative nematic but at low frequency $\epsilon_{\|} > \epsilon_{\perp}$. These observations are not limited to this particular dopant or the particular class of nematic compounds. Figure 3 shows $\epsilon_{app}(v)$ for MBBA doped with dodecylpyridinium-*p*-toluene sulfonate while Fig. 4 shows results for doped chlorostilbenes.† Thus for negative nematics of the azomethine or stilbene type one has $\rho_{\|} < \rho_{\perp}$ and $\epsilon_{app\|} < \epsilon_{app\perp}$ at high frequency but $\epsilon_{app\|} > \epsilon_{app\perp}$ at low frequency. However, for positive azomethines the sign of $\Delta\epsilon$ does not reverse. Figure 5 represents data for alkoxy benzilidene-amino-benzonitrils.

† Samples were prepared by W. R. Young.

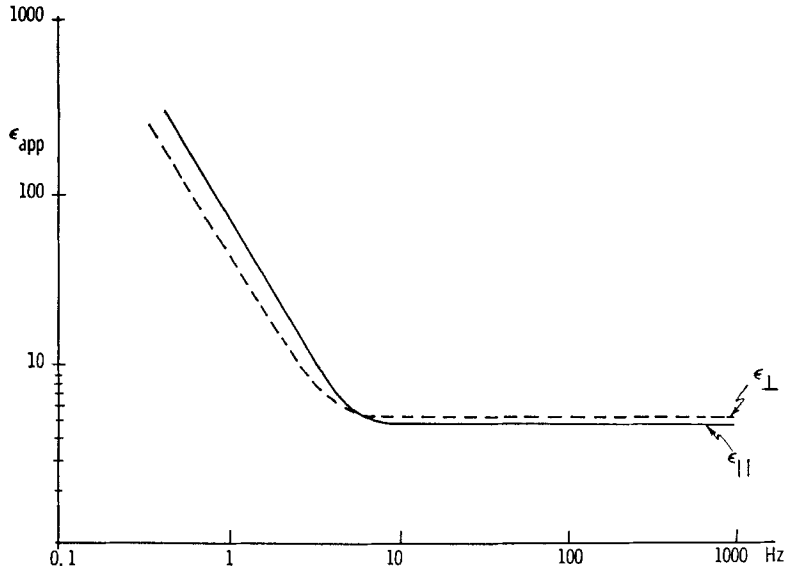

Figure 4. Apparent permittivity of doped chloro-*t*-stilbene mixture.[8]
$\rho_{||} = 0.9 \times 10^9\ \Omega\,\text{cm}$ $\rho_\perp = 1.3 \times 10^9\ \Omega\,\text{cm}$

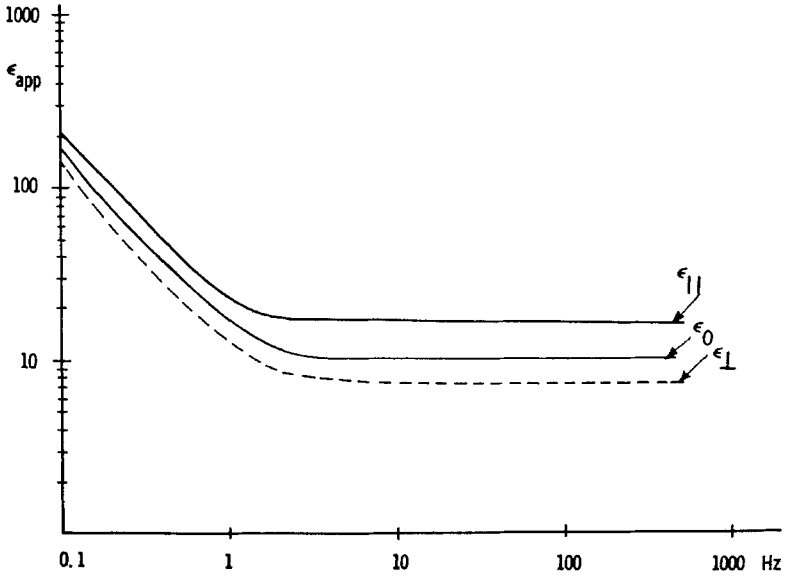

Figure 5. Apparent permittivity of positive nematics. 1 : 1 : 1 molar mixture of butoxy-, hexyloxy-, and heptanoyloxy-benzilidene-amino-benzonitril.
$\rho_{||} = 0.80 \times 10^{10}\ \Omega\,\text{cm}$ $\rho_\perp = 1.1 \times 10^{10}\ \Omega\,\text{cm}$

4. Discussion

Johnson and Cole[5] observed a large increase in the permittivity of formic acid below 10^3–10^4 Hz. It was assumed that there is an electrode impedance in series with the dielectric. Dansas and Sixou[6] found similar behavior for N-ethyl-acetamide and finally, Heilmeier[7] briefly indicated his results for *p*-azoxyanisole without further discussion.

All results can be accounted for by introducing an electrode capacitance assumed to be the capacitance of a double layer of ions absorbed on the electrode surface and a diffuse layer of counter ions in the liquid. The cell is now characterized by a capacitance C_{el} in series with the parallel combination of the bulk capacitance and resistance. However, the bridge still interprets this as a parallel RC network. Let the index " m " denote the measured parameter, then one has, by equating the real and imaginary parts of Eqs. 1 and 2:

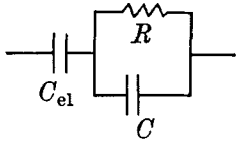

$$Z = \frac{R(1 - j\omega RC)}{1 + (\omega RC)^2} + \frac{1}{j\omega C_{el}} \tag{1}$$

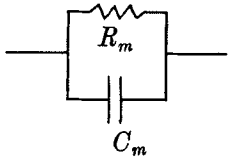

$$Z_m = \frac{R_m(1 - j\omega R_m C_m)}{1 + (\omega R_m C_m)^2} \tag{2}$$

$$\frac{R_m}{1 + (\omega R_m C_m)^2} = \frac{R}{1 + (\omega RC)^2} \tag{3}$$

$$\frac{1}{C_m} \cdot \frac{(\omega R_m C_m)^2}{1 + (\omega R_m C_m)^2} = \frac{1}{C} \cdot \frac{(\omega RC)^2}{1 + (\omega RC)^2} + \frac{1}{C_{el}} \tag{4}$$

For $\omega R_m C_m \ll 1$ Eqs. (3) and (4) simplify to:

$$R_m \approx R \tag{5}$$

$$\omega^2 R_m^2 (C_m - C) C_{el} \approx 1 \tag{6}$$

while for $\omega R_m C_m \gg 1$ one has

$$R_m \approx R \tag{7}$$

$$\frac{1}{C_m} \approx \frac{1}{C} + \frac{1}{C_{el}} \approx \frac{1}{C} \tag{8}$$

The cell resistance is approximately equal to R_m throughout the frequency range. The electrode capacitance is obtained from Eq. 6. At frequencies well below the knee in the $\epsilon(\upsilon)$ curve $C \ll C_m$ and Eq. 6 simplifies further to:

$$C_{el} \approx \frac{C_m}{(\omega R_m C_m)^2} \gg C_m \tag{9}$$

The electrode capacitance is much larger than the bulk capacitance and thus at frequencies well beyond the knee of the $\epsilon(\upsilon)$ curve $C_m \approx C$ as in Eq. 8.

Data for C_{el} calculated from Eq. 6 for the sample in Fig. 2 are collected kn Table 1.

TABLE 1 Electrode Capacitance in $\mu F/cm^2$

Hz	C_{el} ∥	C_{el} ⊥	$\epsilon_{\parallel}/\epsilon_{\perp}$	$(\rho_{\perp}/\rho_{\parallel})^2$
0.2	1.41	1.49	2.4	2.4
1.5	1.30	1.30	2.4	2.4
1	1.23	1.25	2.4	2.4
2	1.11	1.14	2.4	2.4

C_{el} is the equivalent capacitance used in the equations. Assuming that both electrodes are identical the capacitance at each electrode would of course be twice the values in the table.

It is seen that C_{el} does not depend on the direction of the magnetic field, adsorption is not affected by the magnetic field. It follows that in the range of frequency where Eq. (9) can be used:

$$\left(\frac{\epsilon_{\parallel}}{\epsilon_{\perp}}\right)_{app} = \left(\frac{\rho_{\perp}}{\rho_{\parallel}}\right)^2 \tag{10}$$

for constant ω.

Experimental data are found to satisfy Eq. 10 for both positive and negative nematics, see Table 1. Since the ratio $(\rho_{\perp}/\rho_{\parallel})^2 > 1$ for

positive as well as negative mesogens, Eq. 10 requires that $\epsilon_{\parallel} > \epsilon_{\perp}$ for both types at sufficiently low frequency. But since $\epsilon_{\parallel} < \epsilon_{\perp}$ for negative nematics at high frequency the $\epsilon_{\parallel}(\upsilon)$ and $\epsilon_{\perp}(\upsilon)$ curves must intersect at some frequency. However, for positive nematics the $\epsilon(\upsilon)$ curves do not intersect.

The magnitude of C_{el} depends on the type of dopant and its concentration but not on the alignment of the nematic host material. Thus C_{el} is invariant to an external magnetic field and a curve of C_{el} versus temperature does not show a discontinuity at the N–I transformation temperatures. See Fig. 6.

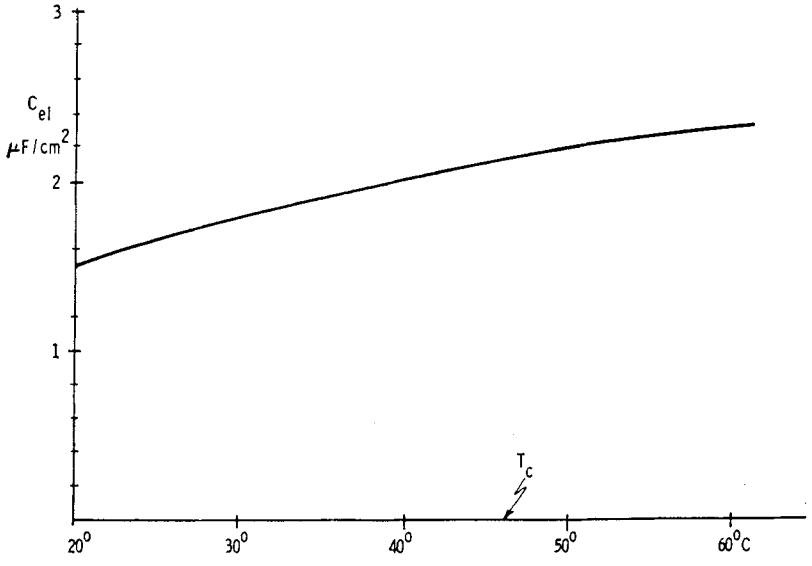

Figure 6. Surface capacitance C_{el} in $\mu F/cm^2$ for doped MBBA as function of temperature. There is no discontinuity at T_c.

The Electrode Space Charge

The experimental data can be accounted for by a three parameter model :

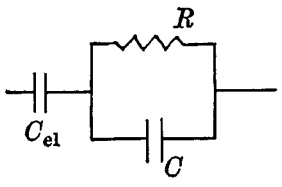

The cell resistance R is in the range 0.1–50 mΩ/cm^2 for 0.001 in. spacing, depending on the doping concentration. The cell capacitance C is about 220 pF/cm^2 for MBBA. The electrode capacitance C_{el} is in the range 0.5–5 μF/cm^2 again depending on the type of dopant and its concentration. R and C are independent of frequency in the range 0.1 Hz to 10 kHz. C_{el} can be determined accurately only at low frequencies, it is a weak function of the frequency. It remains to justify C_{el} on a molecular basis.

From Gouy–Chapman theory[9] the surface charge of a double layer is:

$$\sigma = \frac{\epsilon\chi}{2\pi} \cdot \frac{kT}{e} \cdot \sinh \frac{e\psi}{2kT} \tag{11}$$

in which the Debye length $1/\chi$ is determined by

$$\chi^2 = \frac{8\pi n e^2}{\epsilon kT} \tag{12}$$

ψ is the potential drop across the diffuse layer,

$$\psi_\infty = 0 \text{ and } (\partial\psi/\partial x)_\infty = 0.$$

From Eq. 11 the space charge capacitance is

$$\frac{d\sigma}{d\psi} = \frac{\epsilon\chi}{4\pi} \cosh \frac{e\psi}{2kT} \tag{13}$$

If one identifies $d\sigma/d\psi$ with the observed capacitance C_{el} and the potential ψ with the voltage across C_{el} in the series circuit C_{el}, R an estimate of the double layer parameters and the dissociation constant can be obtained.

Using data in Fig. 4 and Table 1 as an example, at 0.2 Hz $C_{el} = 1.4$ μF/cm^2, $V = 1$ volt, and $R = 1.5$ m Ω/cm^2 and thus:

$$\psi = (1 + \omega^2 R^2 C^2)^{-1/2} \; V = 0.37 \text{ volt}$$

From Eq. (13) one obtains:

$$\chi = 1.8 \times 10^{-5} \text{ cm}^{-1}$$

and hence the double layer width is of the order of 500 Å.

Using this value of χ in Eq. (12) the concentration of charge carriers, n, is obtained and by comparing n with the dopant concentration one finds the degree of dissociation α, of the dopant

$$\alpha = 0.6 \times 10^{-2}.$$

Finally the surface charge density σ is calculated from 11

$$\sigma = 0.3 \times 10^{-6} \text{ coulomb/cm}^2$$

corresponding to about 10^{12} ions/cm^2.

The field in the double layer near the surface is of the order of 10^4 volt/cm. The order of magnitude of the parameters χ, σ, and α is acceptable and thus C_{el} can be interpreted as the capacitance of the double layer. However, the model is too crude to expect more than order of magnitude results. A well-known weakness of the Gouy–Chapman model is the fact that ψ is not an experimental quantity, see Ref. 9. Moreover carrier transport by diffusion and drift is neglected. To illustrate the deficiency of the model, if ψ is identified with V_c the differential capacitance $d\sigma/d\psi$ would decrease as v increases to a limiting value $\epsilon\chi/4\pi$. Indeed C_{el} is found to decrease with increasing v but at a much lower rate.

5. Summary

It has been shown that the experimental data can be accounted for by an impedance as in Eq. (1), which is interpreted as the impedance of a surface capacitance in series with the bulk resistance and bulk capacitance.

The cell resistance is independent of the frequency in the range 0.1 Hz to 10 kHz, it can be varied from 50 to 0.1 mΩ/cm^2 (for 1 mil cells) by adding dopants. The cell capacitance is of the order of 200 pF/cm^2 for 1 mil cells. It is independant of frequency and changes slightly by adding dopants.

The electrode capacitance is of the order of 0.5–5 μF/cm^2 and depends strongly on the dopant. It decreases slightly with increasing frequency.

Acknowledgements

The cooperation of J. Overmeyer is gratefully acknowledged. W. R. Young prepared the chloro stilbene sample used in Fig. 6.

REFERENCES

1. Diguet, D., Rondolez, F. and Durand, G., *Comp. Rendus Acad. Sci.* **271B** 954 (1970).

2. Heilmeier, G. H., Zanoni, L. A. and Barton L. A., *IEEE*, E.D.–**17**, 22 (1970).
3. Schadt, M., *J. Chem. Phys.* **56**, 1494 (1972).
4. Sprokel, G. J., Elect. Chem. Soc. Meeting, Miami, Fla. 1972.
5. Johnson, J. F. and Cole, R. H., *J.A.C.S.* **73**, 4536 (1951).
6. Dansas, P. and Sixou, P., *Rev. Gen de l'Ectricite* **76**, 726 (1967).
7. Heilmeier, G. H., *J. Chem. Phys.* **44**, 644 (1966).
8. Young, W. R., Aviram, A. and Cox, R. J., *Angew. Chem.* **83**, 399 (1971).
9. The Gouy-Chapman Theory is discussed in many textbooks. The terminology used here is taken from Chapter IV of Overbeek, J. Th. G., *Kruyt Colloid Science*, Elsevier, 1952. See also J. Ross Macdonald and C. A. Barlow, *First Conf. on Electrochemistry*, Pergamon, 1965, pp. 199–247.